

## 2. DIFFRACTION GEOMETRY AND ITS PRACTICAL REALIZATION

The method can also be used with a receiving slit or position-sensitive detectors (Lehmann *et al.*, 1987; Shishiguchi, Minato & Hashizume, 1986). The latter can be a short straight detector, which can be scanned to increase the data-collection speed (Göbel, 1982), or a longer curved detector.

## 2.3.2.3. Grazing-incidence diffraction

In conventional focusing geometry, the specimen and detector are coupled in  $\theta$ - $2\theta$  relation at all  $2\theta$ 's to avoid defocusing and profile broadening. In Seemann-Bohlin geometry, changing the specimen position necessitates realigning the diffractometer and very small incidence angles are inaccessible. In parallel-beam geometry, the specimen and detector positions can be uncoupled without loss of resolution. This freedom makes possible the use of different geometries for new applications. The specimen can be set at any angle from grazing incidence to slightly less than  $2\theta$ , and the detector scanned. Because the incident and exit angles are unequal, the relative intensities may differ by small amounts from those of the  $\theta$ - $2\theta$  scan due to specimen absorption. The reflections occur from differently oriented crystallites whose planes are inclined (rather than parallel) to the specimen surface so that particle statistics becomes an important factor. The method is thus similar to Seemann-Bohlin but without focusing.

The method can be used for depth-profiling analysis of polycrystalline thin films using grazing-incidence diffraction (GID) (Lim, Parrish, Ortiz, Bellotto & Hart, 1987). If the angle of incidence  $\theta_i$  is less than the critical angle of total reflection  $\theta_c$ , diffraction occurs only from the top 35 to 60 Å of the film. Comparison of the GID pattern with a conventional  $\theta$ - $2\theta$  pattern in which the penetration is much greater gives structural information for phase identification as a function of film depth. The intrinsic profile shapes are the same in the two patterns and broadening may indicate smaller particle sizes. However, if the film is epitaxial or highly oriented, it may not be possible to obtain a GID pattern.

For  $\theta_i < \theta_c$ , the penetration depth  $t'$  is (Vineyard, 1982)

$$t' \simeq \lambda / [2\pi(\theta_c^2 - \theta_i^2)^{1/2}] \quad (2.3.2.1)$$

and, for  $\theta_i > \theta_c$ ,

$$t' \simeq 2\theta_i / \mu, \quad (2.3.2.2)$$

where  $\mu$  is the linear absorption coefficient. The thinnest top layer of the film that can be sampled is determined by the film density, which may be less than the bulk value. As  $\theta_i$  approaches  $\theta_c$ , the penetration depth increases rapidly and fine control becomes more difficult. Fig. 2.3.2.7 shows this relation and the advantage of using longer wavelengths for a wider range of penetration control. For example, for a film with  $\mu = 200 \text{ cm}^{-1}$ ,  $\lambda = 1.75 \text{ \AA}$ , and  $\theta_i = 0.1^\circ$ , only the top 45 Å contribute, and increasing  $\theta_i$  to  $0.35^\circ$  increases the depth to 130 Å. The patterns have much lower intensity than a  $\theta$ - $2\theta$  scan because of the smaller diffracting volume.

Fig. 2.3.2.8 shows patterns of a 5000 Å polycrystalline film of iron oxide deposited on a glass substrate and recorded with (a)  $\theta$ - $2\theta$  scanning and (b)  $0.25^\circ$  GID. The film has preferred orientation as shown by the numbers above the peaks in (a), which are the relative intensities of a random powder sample. The relative intensities are different because in (a) they come from planes oriented parallel to the surface and in (b) the planes are inclined. The glass scattering that is prominent in (a) is absent in (b) because the beam does not penetrate to the substrate.

## 2.3.2.4. High-resolution energy-dispersive diffraction

By step scanning the channel monochromator instead of the specimen, a different wavelength reaches the specimen at each step and the pattern is a plot of intensity versus wavelength or energy (Parrish & Hart, 1985, 1987). The X-ray optics can be the same as described in Subsection 2.3.2.1 and determines the resolution. A scintillation counter with conventional electronic circuits can be used. As in the conventional white-beam energy-

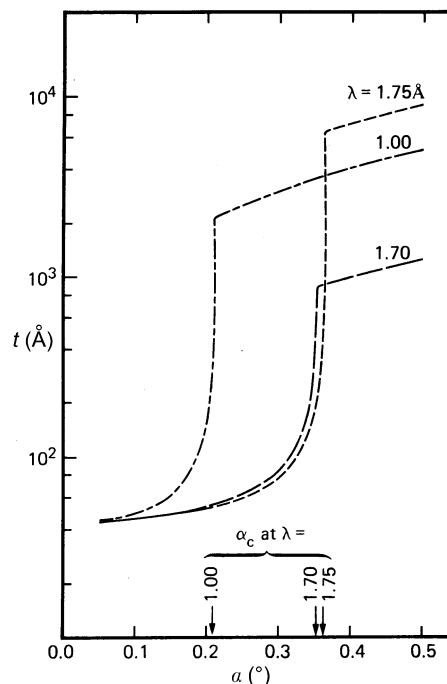


Fig. 2.3.2.7. Penetration depth  $t'$  as a function of grazing-incidence angle  $\alpha$  for  $\gamma\text{-Fe}_2\text{O}_3$  thin film. The critical angle of total reflection  $\alpha_c$  is shown by the vertical arrows for different wavelengths.

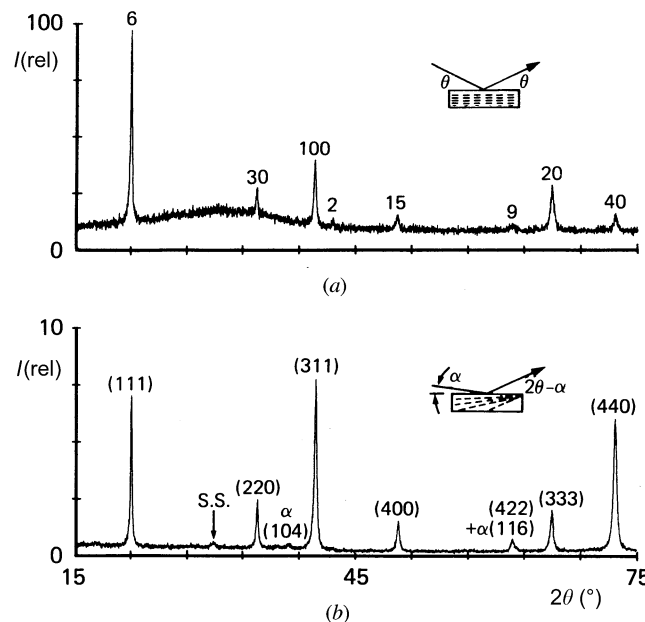


Fig. 2.3.2.8. Synchrotron diffraction patterns of annealed 5000 Å iron oxide film,  $\lambda = 1.75 \text{ \AA}$ , (a)  $\theta$ - $2\theta$  scan; relative intensities of random powder sample shown above each reflection. (b) Grazing incidence pattern of same film with  $\alpha = 0.25^\circ$  showing only reflections from top 60 Å of film, superstructure peak S.S. and  $\alpha\text{-Fe}_2\text{O}_3$  peaks not seen in (a). Absolute intensity is an order of magnitude lower than (a).

### 2.3. POWDER AND RELATED TECHNIQUES: X-RAY TECHNIQUES

dispersive diffraction (EDD) described in Section 2.5.1, the specimen and detector remain fixed at selected angles during the recording. This makes it possible to design special experiments that would not be possible with specimen-scanning methods. It also simplifies the design of specimen-environment chambers for high and low temperatures. The advantages of the method over conventional EDD are the order-of-magnitude higher resolution that can be controlled by the X-ray optics, the ability to handle high peak count rates with a high-speed scintillation counter and conventional circuits, and much lower count times for good statistical accuracy.

The accessible range of  $d$ 's that can be recorded using a selected wavelength range is determined by the  $2\theta$  setting of the detector. Changing  $2\theta$  causes the separation of the peaks to expand or compress in a manner similar to a variation of  $\lambda$  in conventional diffractometry. This is illustrated in Figs. 2.3.2.9(a)–(d) for a quartz powder specimen using an Si(111) channel monochromator and  $\theta_M = 19$  to  $5^\circ$  (2.04 to 0.55 Å, 6.1

to 22.7 keV) and four detector  $2\theta$  settings. At small  $2\theta$  settings, only the large  $d$ 's are recorded and the peak separation is large. Increasing the  $2\theta$  setting decreases the  $d$  range and the separation of the peaks as shown in Fig. 2.3.2.9(e). These patterns were recorded with the pulse-height analyser set to discriminate only against scintillation counter noise.

For given X-ray optics, the profiles symmetrically broaden with decreasing X-ray photon energy and with  $\theta$ . This type of broadening remains symmetrical if  $E$  is increased and  $2\theta$  decreased, or *vice versa*, Fig. 2.3.2.9(f). The two profiles shown have been broadened by the X-ray optics but the intrinsic resolution is far better. The number of points recorded per profile thus decreases with decreasing profile width since  $\Delta\theta_M$  is constant. At the higher energies, it may be desirable to use smaller  $\Delta\theta_M$  steps to increase the number of points to define better the profile. Alternatively, increments in  $\sin\theta$  steps rather than  $\theta$  steps would eliminate this variation.

Many electronic solid-state devices use thin films that are purposely prepared to have single-crystal structure (*e.g.* epitaxial growth), or with a selected lattice plane oriented parallel or normal to the film surface to enhance certain properties. The properties vary with the degree of orientation and textural characterization is essential to make the correct film preparation. Preferred orientation can be detected by comparing the relative intensities of the thin-film pattern with those of a random powder. The pattern can be recorded with conventional  $\theta$ - $2\theta$  scanning ( $\lambda$  fixed) or by EDD. However, this only gives information on the planes oriented parallel to the surface. To study inclined planes requires uncoupling the specimen surface and detector angles. This can be done with the EDD method described above without distorting the profiles (Hart *et al.*, 1987).

The principle of the method is illustrated in Fig. 2.3.2.10. The set of lattice planes ( $hkl$ ) oriented parallel to the surface has its highest intensity in the symmetric  $\theta$ - $2\theta$  position. Rotating the specimen by an angle  $\theta_r$  while keeping  $2\theta$  fixed reduces the intensity of ( $hkl$ ) and brings another set of planes ( $pqr$ ), which are inclined to the surface, to its symmetrical reflecting position. The required rotation is determined by the interplanar angle between ( $hkl$ ) and ( $pqr$ ). The angular distribution of any plane can be measured with respect to the film surface by step scanning at small  $\theta_r$  steps. The specimen is rotated clockwise with the limitation  $\theta_s + \theta_r < 2\theta$ . A computer automation program is desirable for large numbers of measurements.

Fig. 2.3.2.3(c) shows the appearance of a pattern of a specimen containing elements with absorption edges in the recording range and using electronic discrimination only against electronic noise. Starting at the incident high-energy side, the Zn and Ni K fluorescence increases as the energy approaches the edges ( $\lambda^3$  law), decreases abruptly when the energy crosses each edge, and disappears beyond the Ni K edge. Long-wavelength fluorescence is absorbed in the windows and air path.

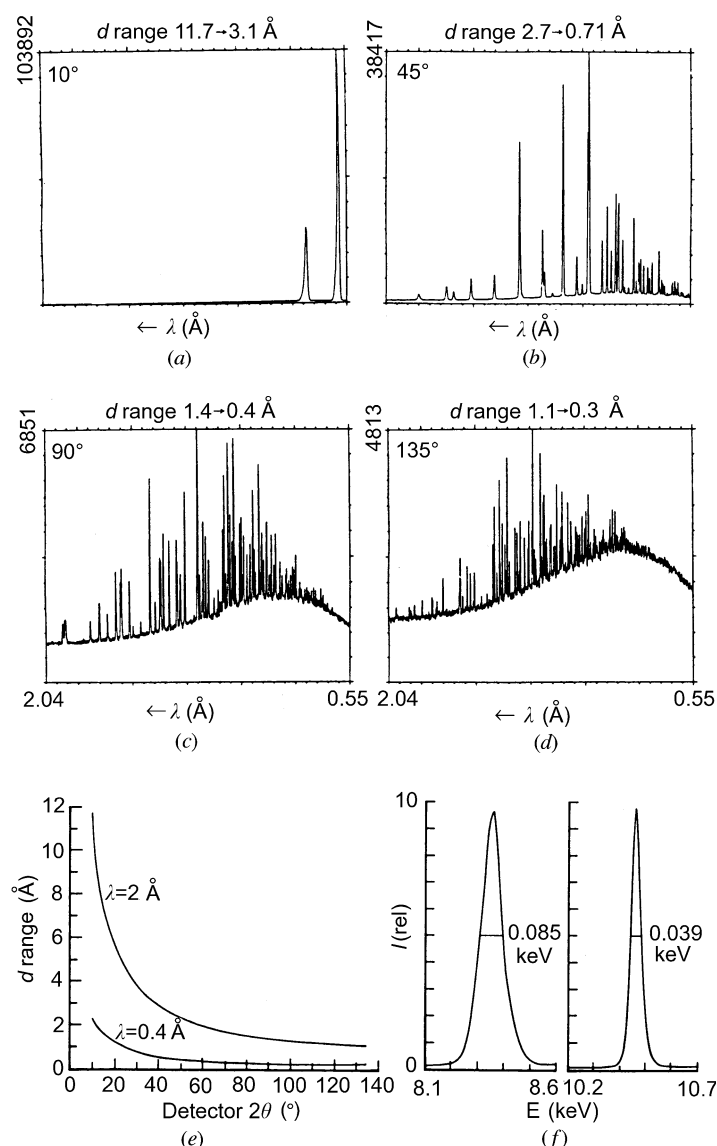


Fig. 2.3.2.9. (a)–(d) High-resolution energy-dispersive diffraction patterns of quartz powder sample obtained with  $2\theta$  settings shown in upper left corners. (e)  $d$  range as a function of detector  $2\theta$  setting for  $\lambda = 0.4$  to  $2$  Å. (f) Effect of  $2\theta$  setting and  $E$  on profile widths of quartz. Right: 121 reflection,  $20^\circ 2\theta$ ,  $E_p$  10.45 keV; left: 100 reflection,  $45^\circ 2\theta$ ,  $E_p$  8.35; both reflections broadened by X-ray optics and peak intensity of 100 twice that of 121.

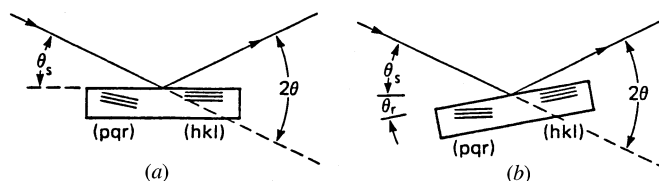


Fig. 2.3.2.10. Specimen orientation for symmetric reflection (a) from ( $hkl$ ) planes and (b) specimen rotated  $\theta_r$  for symmetric reflection from ( $pqr$ ) planes.

## 2. DIFFRACTION GEOMETRY AND ITS PRACTICAL REALIZATION

The method is of doubtful use for structure determination or quantitative analysis. The wide range of wavelengths, continually varying absorption and profile widths, and other factors create a major difficulty in deriving accurate values of the relative intensities.

Conventional energy-dispersive diffraction methods using white X-rays and a solid-state detector are described in Chapter 2.5 and Section 5.2.7.

### 2.3.3. Specimen factors, angle, intensity, and profile-shape measurement

The basic experimental procedure in powder diffraction is the measurement of intensity as a function of scattering angle. The profile shapes and  $2\theta$  angles are derived from the observed intensities and hence the counting statistical accuracy has an important role. There is a wide range of precision requirements depending on the application and many factors are involved: instrument factors, counting statistics, profile shape, and particle-size statistics of the specimen. *The quality of the specimen preparation is often the most important factor in determining the precision of powder diffraction data.*

D. K. Smith and colleagues (see, for example, Borg & Smith, 1969; see also Yvon, Jeitschko & Parthé, 1977) developed a method for calculating theoretical powder patterns from well determined single-crystal structures and have made available a Fortran program (Smith, Nichols & Zolensky, 1983). This has important uses in powder diffraction studies because it provides reference data with correct  $I$ 's and  $d$ 's, free of sample defects, preferred orientation, statistical errors, and other factors. The data can be displayed as recorded patterns by using plot parameters corresponding to the experimental conditions (Subsection 2.3.3.9). Calculated patterns have been used in a large variety of studies such as identification standards, computing intermediate members of an isomorphous series, testing structure models, ordered and disordered structures, and others. Many experiments can be performed with simulated patterns to plan and guide research. The method must be used with some care because it is based on the small single crystal used in the crystal-structure determination and the large powder samples of minerals and ceramics, for example, may have a different composition. Errors in the structure analysis are magnified because the powder intensities are based on the squares of the structure factors.

The Lorentz and polarization factors for diffractometry geometry have been discussed by Ladell (1961) and Pike & Ladell (1961).

Smith & Snyder (1979) have developed a criterion for rating the quality of powder patterns; see also de Wolff (1968a).

#### 2.3.3.1. Specimen factors

Ideally, the specimen should contain a large number of small equal-sized randomly oriented particles. The surface must be flat and smooth to avoid microabsorption effects, *i.e.* particle interferences which reduce the intensities of the incident and reflected beams and can lead to significant errors (Cline & Snyder, 1983). The specimen should be homogeneous, particularly if it is a mixture or if a standard has been added. Low packing density and specimen-surface displacement (§2.3.1.1.6) may cause significant errors. It is recommended that the powder and the prepared specimen be examined with a low-power binocular optical microscope. Smith & Barrett (1979), Jenkins, Fawcett, Smith, Visser, Morris & Frevel (1986), and Bish & Reynolds (1989) have surveyed methods of specimen preparation

and they include bibliographies on special handling problems. Powder diffraction standards for angle and intensity calibration are described in Section 5.2.9.

#### 2.3.3.1.1. Preferred orientation

Preferred orientation changes the relative intensities from those obtained with a randomly oriented powder sample. It occurs in materials that have good cleavage or a morphology that is platy, acicular or any special shape in which the particles tend to orient themselves in specimen preparation. The micas and clay minerals are examples of materials that exhibit very strong preferred orientation. When they are prepared as reflection specimens, the basal reflections dominate the pattern. It is common in prepared thin films where preferred orientation occurs frequently or may be purposely induced to enhance certain optical, electrical, or magnetic properties for electronic devices. By comparison of the relative intensities with the random powder pattern, the degree of preferred orientation can be observed.

Powder reflections take place from crystallites oriented in different ways in the instrument geometries as shown in Fig. 2.3.1.2. In reflection specimen geometry with  $\theta$ - $2\theta$  scanning, reflections can occur only from lattice planes parallel to the surface and in the transmission mode they must be normal to the surface. In the Seemann-Bohlin and fixed specimen with  $2\theta$  scanning methods, the orientation varies from parallel to about  $45^\circ$  inclination to the surface. The effect of preferred orientation can be seen in diffraction patterns obtained by using the same specimen in the different geometries.

The effect is illustrated in Fig. 2.3.3.1 for *m*-chlorobenzoic acid,  $C_7H_5ClO_2$ , with reflection and transmission patterns and the pattern calculated from the crystal structure. The degree of preferred orientation is shown by comparing the peak intensities of four reflections in the three patterns:

(hkl)	(120)	(200)	(040)	(121)
Reflection	9.8	0.6	1.6	2.5
Transmission	5.2	0.5	0.7	9.3
Calculated	3.0	6.6	4.0	9.1.

Care is required to make certain the differences are not caused by a few fortuitously oriented large particles.

Various methods have been used to minimize preferred orientation in the specimen preparation (Calvert, Sirianni, Gainsford & Hubbard, 1983; Smith & Barrett, 1979; Jenkins *et al.*, 1986; Bish & Reynolds, 1989). These include using small particles, loading the powder from the back or side of the specimen holder, and cutting shallow grooves to roughen the surface. The powder has also been sifted directly on the surface of a microscope slide or single-crystal plate that has been wetted with the binder or petroleum jelly. Another method is to mix the powder with an inert amorphous powder such as Lindemann glass or rice starch, or add gum arabic, which after setting can be reground to obtain irregular particles. Any additive reduces the intensity and the peak-to-background ratio of the pattern. A promising method that requires a considerable amount of powder is to mix it with a binder and to use spray drying to encapsulate the particles into small spheres which are then used to prepare the specimen (Smith, Snyder & Brownell, 1979).

Preferred orientation would not cause a serious problem in routine identification providing the reference standard had a similar preferred orientation and both patterns were obtained with the same diffractometer geometry. However, when accurate values of the relative intensities are required, as in crystal-